Nuclear Engineering and Technology 53 (2021) 715–731

Contents lists available at ScienceDirect

Nuclear Engineering and Technology

journal homepage: www.elsevier.com/locate/net

Original Article

Uncertainty quantification of PWR spent fuel due to nuclear data and modeling parameters

Bamidele Ebiwonjumi, Chidong Kong, Peng Zhang, Alexey Cherezov, Deokjung Lee*

Department of Nuclear Engineering, Ulsan National Institute of Science and Technology, 50 UNIST-gil, Ulsan, 44919, Republic of Korea

ARTICLE INFO

Article history:
Received 6 April 2020
Received in revised form
3 July 2020
Accepted 11 July 2020
Available online 26 July 2020

Keywords:
STREAM
Spent nuclear fuel
PWR
Uncertainty quantification
Stochastic sampling
Surrogate models

ABSTRACT

Uncertainties are calculated for pressurized water reactor (PWR) spent nuclear fuel (SNF) characteristics. The deterministic code STREAM is currently being used as an SNF analysis tool to obtain isotopic inventory, radioactivity, decay heat, neutron and gamma source strengths. The SNF analysis capability of STREAM was recently validated. However, the uncertainty analysis is yet to be conducted. To estimate the uncertainty due to nuclear data, STREAM is used to perturb nuclear cross section (XS) and resonance integral (RI) libraries produced by NJOY99. The perturbation of XS and RI involves the stochastic sampling of ENDF/B-VII.1 covariance data. To estimate the uncertainty due to modeling parameters (fuel design and irradiation history), surrogate models are built based on polynomial chaos expansion (PCE) and variance-based sensitivity indices (*i.e.*, Sobol' indices) are employed to perform global sensitivity analysis (GSA). The calculation results indicate that uncertainty of SNF due to modeling parameters are also very important and as a result can contribute significantly to the difference of uncertainties due to nuclear data and modeling parameters. In addition, the surrogate model offers a computationally efficient approach with significantly reduced computation time, to accurately evaluate uncertainties of SNF integral characteristics.

1. Introduction

The radiation source terms of spent nuclear fuel (SNF) needs to be characterized for safety applications in the back-end of the fuel cycle. SNF pools around the world are getting closer to saturation and it is difficult to measure the characteristics of all discharged fuels from nuclear reactors. Thus, the determination of the source terms depends largely on predictions of computer codes which model nuclide depletion during irradiation in the reactor core and decay during cooling or after discharge. The Steady state and Transient Reactor Analysis code with Method of Characteristics (STREAM) has been developed to perform light water reactor (LWR) whole core analysis [1] including support for SNF applications, deep penetration problems, radiation shielding and cask analysis [2]. STREAM depletion and source term calculation capabilities have been validated against measurement data of SNF isotopic compositions [3] and fuel assembly (FA) decay heat [4]. However, the uncertainty quantification (UQ) is yet to be conducted. UQ of calculated source terms is essential to assess the accuracy and reliability of code predictions. Over the years, several approaches have been developed to perform UQ and sensitivity analysis (SA). Examples include perturbation method and stochastic sampling (SS) approach which have been implemented in codes including TSUNAMI [5], SAMPLER [6], SHARK-X [7], and XSUSA [8]. In the SS case, the inputs (nuclear data, modeling parameters) considered as uncertain are perturbed and then applied to the computer code of interest in repeated calculations. Then the response of interest is obtained and post-processed to determine the uncertainty due to the perturbed inputs. This approach is known as forward UQ. For the uncertainty due to nuclear data, covariance of nuclear data can be used.

Until now, most of the works carried out on SNF UQ have been based on the propagation of nuclear data uncertainties in SNF characteristics [6,9,10]. Little attention has been paid to uncertainties in SNF due modeling parameters such as fuel design and irradiation history information [11–13]. What references [11–13] focused on includes the modeling parameter induced uncertainties in boiling water reactor (BWR) fuel assembly decay heat, best estimate of ^{244}Cm calculated content in an LWR pin compared to

* Corresponding author.
E-mail addresses: ebiwonjumi@unist.ac.kr (B. Ebiwonjumi), kcd1006@unist.ac.kr (C. Kong), zhangpeng@unist.ac.kr (P. Zhang), alcher@unist.ac.kr (A. Cherezov), deokjung@unist.ac.kr (D. Lee).

https://doi.org/10.1016/j.net.2020.07.012

measurement, and calculated contents of isotopic inventory in LWR pin, respectively. To the best of the authors' knowledge, there is a lack of available studies which demonstrates the impact of modeling parameters uncertainties in a pressurized water (PWR) SNF assembly characteristics. This study will quantify uncertainties in calculated PWR SNF characteristics due to both nuclear data and modeling parameters uncertainties. The stochastic sampling approach is computationally expensive due to the large number of repeated calculations that must be performed. To overcome this problem, surrogate models can be developed and validated, to replace computationally expensive calculations. Surrogate models have become very attractive in many areas of science and engineering [14], including reactor physics SA/UQ [15,16], to replace computationally expensive code calculations. The advantages of the surrogate model developed in this work are that they can be developed with small number of reference code calculations or model response evaluations and can be deployed at very small computational cost to provide accurate mapping between the input data and model response. In this work, we perform forward UQ by a non-intrusive approach and a polynomial chaos expansion (PCE) based surrogate model is built for the STREAM code during the process. It should be noted however, that the surrogate models are only used to propagate the modeling parameter uncertainties and the SS approach is used to propagate the nuclear data uncertainties.

A typical PWR fuel assembly following realistic and detailed irradiation history is chosen for the UQ. To propagate the modeling parameter uncertainties, the SA/UQ is performed by the UQ tool UQLAB which contains the implementation of the PCE based surrogate model [17] and variance-based sensitivity indices in a global sensitivity analysis (GSA). The goal of this study is twofold. The first is to quantify the uncertainties in STREAM predictions of SNF characteristics. The second is to demonstrate that surrogate models and Sobol' indices can be employed in SNF applications to perform global SA and UQ due to modeling parameters. The rest of this paper is arranged as follows. The selected PWR SNF assembly is presented in Section 2 alongside the fuel design, irradiation history and uncertainty information. Section 3 describes the STREAM code, the stochastic sampling of the covariance of nuclear data in STREAM, the PCE based surrogate model and global SA. Section 4 discusses the results of UQ due to modeling parameters and nuclear data uncertainties. The conclusions are summarized in Section 5.

2. Description of the assembly

A Westinghouse 15 × 15 fuel assembly design is used as the test case in this study. This assembly has been selected from a group of assemblies analyzed previously with available decay heat measurements [4] at the Swedish central interim storage facility for spent nuclear fuel, CLAB [18]. The assembly is designated as *C01*, with enrichment of 3.1 wt% ^{235}U, discharge burnup of 36.7 GWd/tU, and active fuel height of 365.8 cm. The assembly contains 204 UO_2 fuel rods, no burnable absorber or poison rod, one instrument tube, 20 guide tubes and the geometry is presented in Fig. 1. The assembly was irradiated in four cycles with a cooling time of about 23 years after discharge before measurement of decay heat. Details of the assembly design and irradiation history information can be obtained from Ref. [18]. Uncertainties in the modeling parameters are obtained from literature [11,12] and shown in Table 1, alongside the nominal values and probability distribution. Details of other unperturbed modeling parameters are summarized in Table 2. In Table 2, the clad thickness will not remain unperturbed. It will be changed due to the perturbation of the clad outer radius. Nevertheless, the clad thickness is not considered as an uncertain model parameter and it is not supplied as one of the inputs of the surrogate model. The uncertainties in Table 1 are assumed to follow a uniform probability distribution. For each input parameter, the same uncertainty value is applied to all the fuel pins. The specific power (*i.e.*, power density used in depletion calculation) is perturbed at the beginning of every cycle where it is defined. The benchmark contains cycle-average power history information for this assembly problem. Other uncertain parameters *e.g.*, fuel/moderator temperature and boron concentration are only perturbed at the beginning of the first cycle. Then the same perturbed values are used in the subsequent cycles. The fuel/moderator temperature and boron concentration are average values over the entire burnup as available in the benchmark. If the benchmark documentation contains the history of fuel/moderator temperature

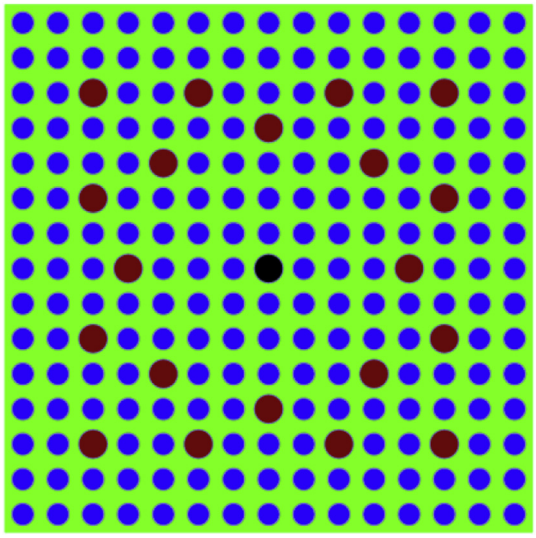

Fig. 1. Layout of C01 PWR assembly. Legend: blue (UO_2), green (moderator), red (guide tube), black (instrument tube). (For interpretation of the references to colour in this figure legend, the reader is referred to the Web version of this article.)

Table 1
Modeling parameters and their uncertainties.

Parameter	Nominal value	Uncertainty (%)	Distribution	Ref.
Fuel density	10.227 g/cc	0.41	Uniform	[11]
^{235}U enrichment	3.095 wt.%	0.54		
Pellet radius	0.4645 cm	0.54		
Clad outer radius	0.5360 cm	1.55		
Fuel temperature	900 K	3.33		
Specific power, cycle 1	10.93 W/g	1.67		
Specific power, cycle 2	35.22 W/g			
Specific power, cycle 3	24.26 W/g			
Specific power, cycle 4	29.20 W/g			
Mod Temp	577 K	2.00		[12]
Boron Conc.	650 ppm	2.00		

Table 2
Other modeling parameters of assembly C01.

Parameter	Nominal value
Assembly pitch	21.50 cm
Rod pitch	1.43 cm
Clad thickness	0.0618 cm
Moderator density	0.72 g/cc
Guide tube outer radius	0.6935 cm
Guide tube inner radius	0.6505 cm
Operating days (4 cycles)	1029/267/312/290
Downtime days	85/56/442

and boron concentration, they can be perturbed every time they are re-defined. It is important to mention that the changes in the modeling parameters caused by the burnup are not considered. This approximation is important because uncertainties in the modeling parameters will be impacted as the burnup progresses. The changes that occur during burnup include bowing and deformation of rods, thermomechanical interactions in the pellet-clad gap, irradiation swelling, and densification effects.

3. Computational models and methods

The description of the computational tools is presented in this section. The deterministic code STREAM performs the depletion and source term calculation to generate the model response. The implementation of the PCE based surrogate model and calculation of Sobol' indices in the global SA is available in the UQ tool, UQLab [17]. STREAM can be coupled to the UQ tool by a scripting interface and system call for single parameter perturbation. Uncertain parameters in STREAM are replaced by the values generated by the UQ tool. For multiple parameter perturbation, the replacement of uncertain parameters was done by post-processing. Latin Hypercube Sampling (LHS) has been employed assuming a uniform distribution with mean, and standard deviation shown in Table 1 to generate perturbed samples of the uncertain modeling parameters. Although there are correlations between the input parameters in Table 1, these correlations are not accounted for in the uncertainty analysis.

3.1. STREAM

STREAM is an LWR analysis tool with lattice physics capabilities, neutron transport and depletion solver. STREAM uses 72-group cross sections and the pin-based slowing-down method (PSM) [19] to generate effective multi-group cross sections. Self-shielding in the resolved resonance region is performed by solving the transport equation with collision probabilities for pin-cell. Neutron transport solution is based on the method of characteristics (MOC), adopting the assembly-modular ray tracing technique to discretize the ray tracing information and T-Y optimum quadrature set to discretize the polar angles, for computational efficiency. The anisotropic scattering is treated with the inflow transport corrected P0 model [20]. The Depletion equation is solved by the Chebyshev Rational Approximation Method (CRAM) and ENDF/B-VII.1 nuclear data library is used in this work. A two-dimensional (2D) model with reflective boundary condition is used in the assembly calculation. STREAM depletion calculation for the assembly test case was modeled with the irradiation history of Tables 1 and 2 in 67 burnup steps.

3.1.1. Stochastic sampling in STREAM

The stochastic sampling of nuclear data implemented in STREAM is discussed in this section. Nuclear microscopic cross section (XS) and resonance integral (RI) libraries are produced by NJOY99. In addition, NJOY99 is used to calculate the multigroup covariance matrix of microscopic cross section of nuclides using the evaluated nuclear data file ENDF/B-VII.1. Then by SS, the covariance matrix is used to randomly perturb the multigroup microscopic cross sections. The perturbed multigroup cross section libraries are prepared to be used in STREAM neutronic calculation. When sampling the nuclear cross sections, the following covariances of multigroup cross sections are considered: the covariance between scattering cross sections, covariance between scattering and fission cross sections, covariance between scattering and capture cross sections, covariance between fission cross sections, covariance between fission and capture cross sections, covariance between capture cross sections, covariance between number of neutrons generated per fission, and covariance between fission spectra. The variances and covariances constitute the diagonal and off-diagonal elements of the covariance matrix. The covariances are the correlated uncertainties. The covariance between different nuclides is not considered. The uncertainties of the microscopic cross sections are assumed to follow the normal distribution. The process of taking correlation into account when sampling the nuclear cross sections is summarized as follows: after NJOY99 calculation of the unperturbed cross sections and the covariance matrix, we performed LHS from a multivariate standard normal distribution. The mean is the unperturbed cross section. The variance and covariances come from the singular value decomposition (SVD) of the covariance matrix. This process produces perturbation factors which are then multiplied with the unperturbed cross sections to generate perturbed cross sections. The entire process is repeated for all microscopic cross sections and all nuclides that have a covariance matrix. Details of the stochastic sampling of the ENDF/B-VII.1 covariance data are not described here but they can be found in the reference [21]. The decay data (half-lives, Q-values) and fission yields are not perturbed, and the effect of their uncertainties are not considered in this study. When the nuclear data uncertainties are propagated in STREAM, the resonance treatment is based on the two-term rational approximation of the equivalence theory [22,23]. Correlations between nuclear data and some of the modeling parameters listed in Table 1 are not considered as such correlations could not be established at the time of this study.

3.2. PCE surrogate model

PCE involves the expansion a given model response $Y(\xi)$ in terms of orthogonal basis functions of uncertain input parameters, vector $\xi = (\xi_1, \xi_2, \ldots, \xi_{n_u})$:

$$Y(\xi) = \sum_{\boldsymbol{n}=0}^{\infty} a_{\boldsymbol{n}} \psi_{\boldsymbol{n}}(\xi) \tag{1}$$

where ξ are the uncertain input parameters, n_u is the number of uncertain input parameters, $\boldsymbol{n}$ is the order of expansion, $a_{\boldsymbol{n}}$ are the expansion coefficients, and $\{\psi_{\boldsymbol{n}}(\xi)\}_0^{\infty}$ represents a complete set of multivariate orthogonal basis in the $L^2(\xi)$ space, being $\xi \in \mathbb{R}^{n_u}$, with inner product:

$$\langle \psi_{\boldsymbol{n}}, \psi_{\boldsymbol{m}} \rangle = \int_{\xi} \psi_{\boldsymbol{n}}(\xi) \psi_{\boldsymbol{m}}(\xi) p(\xi) d\xi \tag{2}$$

where $p(\xi)$ is the joint probability density function (PDF) of all uncertain input parameters. As we will show later, the subscript of the multivariate basis function $\psi_{\boldsymbol{m}}$, has multiple indices $\boldsymbol{m} = (m_1, m_2, \ldots, m_{n_u})$ when expressed in the univariate basis φ_{m_n}. This is to represent the polynomial order and the random variable ξ_n considered in the univariate basis. The terms representing the vector of uncertain input parameters, the expansion order of the PCE coefficients, and order of the multivariate basis are in bold italicized variables. Each uncertain input parameter and the expansion order of the univariate basis will be written in non-bold variables. The expansion in Eq. (1) projects the model response into a basis of polynomials which are orthogonal with respect to a weighting function. The weighting function is the PDF of the random independent variable. The uncertain input parameters in Eq. (1) are assumed to be independent with individual PDF $p_n(\xi_n)$ and joint PDF as Eq. (3).

$$p(\xi) = \Pi_{n=1}^{n_u} p_n(\xi_n) \tag{3}$$

The multivariate basis $\psi_{\boldsymbol{m}}(\xi)$ is constructed as the tensor product of orthogonal univariate functions $\varphi_{m_n}(\xi_n)$:

$$\psi_{\boldsymbol{m}}(\xi) \underline{\underline{\text{def}}} \Pi_{n=1}^{n_u} \varphi_{m_n}(\xi_n) \tag{4}$$

$$(\psi_{\boldsymbol{m}}(\xi))_{\boldsymbol{m}=0}^{\infty} \cong (\varphi_{m_1}(\xi_1)\varphi_{m_2}(\xi_2)\ldots\varphi_{m_{n_u}}(\xi_{n_u}))_{m=0}^{q} \tag{5}$$

The orthogonality condition for the multivariate basis allows us to write Eq. (6):

$$\langle \psi_{\boldsymbol{n}}, \psi_{\boldsymbol{m}} \rangle = \delta_{\boldsymbol{nm}} \tag{6}$$

where $\delta_{\boldsymbol{nm}}$ is the Kronecker delta symbol. The basis function to be employed depends on the probability distribution of the uncertain parameters. Legendre and Hermite polynomials are commonly used as basis functions for uniformly and normally distributed random variables, respectively. The series in Eq. (1) is infinite and is usually truncated at a certain order q, then the model response is approximated by Eq. (7).

$$Y(\xi) \cong \Sigma_{n=0}^{q} a_{\boldsymbol{n}} \psi_{\boldsymbol{n}}(\xi) \tag{7}$$

When the expansion coefficients $a_{\boldsymbol{n}}$ are known, they can be used to determine the mean and variance of the model response. The expansion coefficients are determined by linear regression. Eq. (1) can be written as the sum of Eq. (7) and a truncation error ε_{q+1}, and then cast as a linear system:

$$Y(\xi) = \Sigma_{\boldsymbol{n}=0}^{\infty} a_{\boldsymbol{n}} \psi_{\boldsymbol{n}}(\xi) = \Sigma_{\boldsymbol{n}=0}^{q} a_{\boldsymbol{n}} \psi_{\boldsymbol{n}}(\xi) + \varepsilon_{q+1} \tag{8}$$

$$Y(\xi) \equiv \boldsymbol{a}^T \psi(\xi) + \varepsilon_{q+1} \tag{9}$$

The least square minimization of the mean residual error is set up as:

$$\widehat{\boldsymbol{a}} = arg\ min\ \mathbb{E}\left[\left(\boldsymbol{a}^T \psi(\xi) - Y(\xi)\right)^2\right] \tag{10}$$

where the double-struck upper case $\mathbb{E}$ is an operator for the expectation value of the quantity in square brackets, $\psi(\xi) = (\psi_0(\xi), \ldots, \psi_q(\xi))^T$ is the matrix consisting of Legendre polynomials associated with uniformly distributed random variables and $\boldsymbol{a} = (a_0, \ldots, a_q)^T$ is the vector of coefficients. With the uncertain parameters in Table 1 as input random vector $\boldsymbol{E} = (\xi^{(1)}, \ldots, \xi^{(N)})^T$ from sample of size N and $\boldsymbol{R} = (y^{(1)}, \ldots, y^{(N)})^T$ denoting the model responses (*i.e.*, STREAM simulation results) associated with the inputs, the least square solution of Eq. (10) is given as:

$$\widehat{\boldsymbol{a}} = \left(\Psi^T \cdot \Psi\right)^{-1} \left(\Psi^T \cdot \boldsymbol{R}\right) \tag{11}$$

where:

$$\Psi_{ij} = \psi_j\left(\xi^{(i)}\right) \qquad i = 1, \ldots, N;\ j = 0, \ldots, q \tag{12}$$

and Ψ is an N x $(q+1)$ matrix of Legendre polynomial basis built from Eq. (4). The number of unknowns in the linear system is given by $(n_u + q)!/(n_u!q!)$. At least this number of model evaluations are required to solve the linear system for the coefficients. If the number of model evaluations available is greater than this number, then we have an overdetermined system solvable by least square minimization. Details of the PCE method and its implementation can be found in Ref. [24]. Employing Eq. (6) and basis functions with $\psi_0 = 1$, the mean and variance of the model response can be obtained from the PCE coefficients as:

$$\mu = Y(\xi) = a_0\ , \qquad \sigma^2 = (Y(\xi) - \mu)^2 = \Sigma_{n=1}^{a} a_{\boldsymbol{n}}^2 \tag{13}$$

3.3. Global sensitivity analysis

SA quantifies the output uncertainty of a simulation tool due to the sources of uncertainties in the input parameters. Local SA evaluates the output uncertainty caused by small input variation around certain input parameters using the partial derivative of the model. GSA accounts for the whole range of variation and statistical distribution of input parameters to determine the output uncertainty in a statistical framework. GSA in this paper is based on the decomposition of the model and its variance as suggested by Sobol [25]. The contribution of each input parameter to the variance of the output is known as first order Sobol' indices or the main effect. The total Sobol' indices or total effect considers the contribution of each input parameter plus the high order effects which are the interactions with other input parameters. The Sobol' indices can separate the contribution of individual input to the output variance. Therefore, we can consider a case where there is no correlation among the perturbed modeling parameters in the uncertainty analysis. The total Sobol' indices which includes effect of interactions between the input parameters are commented upon in this study for the sake of completeness. The first order and total Sobol' indices are usually enough to know the significant input parameters. The Sobol' indices can be obtained from the post-processing of PCE coefficients [25–27]. In the Sobol decomposition, the variance of the response is decomposed into parts which are contributed by each of the inputs or a group of inputs. For example, the contribution of each input parameter to the variance of the output, *i.e.*, first order Sobol' indices or the main effect, can be written as:

$$S_i = \frac{1}{\sigma^2} \Sigma_{\boldsymbol{n} \in I_i} a_{\boldsymbol{n}}^2 \tag{14}$$

where the index of the summation refers to basis functions depending *only* on one input parameter i. The high order and total Sobol' indices can be obtained in a similar fashion. When the model response is decomposed into summands, each term of the summation can be viewed as a PCE depending on different subsets of the input parameters [26]. Then the coefficients can be grouped by the input parameters that each polynomial basis depends on [27].

4. Results and discussions

The results of the calculated decay heat for the assembly test case is shown in Table 3 based on unperturbed nuclear data, fuel design and irradiation history information. This table also contains

Table 3
Decay heat results of assembly C01 at 23.2 years cooling.

Results	Value
Calculation (W)	417.08
Measurement (W)	415.75
C/E − 1 (%)	0.32
Measurement uncertainty, 1-sigma (%)	1.40
Calculation uncertainty due to nuclear data (%)	0.72
Calculation uncertainty due to modeling parameters (%)	2.02
Overall calculation uncertainty (%)	2.14

the measured decay heat at 23.2 years cooling time, the calculation-experiment comparison, *i.e.*, bias (C/E − 1), the measurement uncertainty, the calculation uncertainties due to nuclear data and modeling parameters, and the overall calculation uncertainty. The uncertainties due to nuclear data and modeling parameters reported in Table 3 have been calculated as relative standard deviation of the results obtained from three hundred (300) STREAM calculations using perturbed nuclear data and modeling parameters, respectively. All standard deviations in this study correspond to 1-sigma value. Table 3 shows that the calculated assembly decay heat is in very good agreement with the measured data. At 23.2 years cooling, the major decay heat contributors are ^{238}Pu (12.15%), ^{241}Am (11.97%), ^{244}Cm (5.65%), ^{90}Sr (5.42%), ^{90}Y (25.86%), ^{137}Cs (7.59%), and ^{137m}Ba (26.39). The number density uncertainties for these nuclides due to nuclear data and modeling parameters uncertainties are shown in Table 4. ^{90}Y and ^{137m}Ba come from the β^- decay of ^{90}Sr and ^{137}Cs, respectively. ^{90}Y and ^{137m}Ba have the same number density uncertainties as their parents, ^{90}Sr and ^{137}Cs, respectively. Thus, only the uncertainties of the daughter products are shown in Table 4. As can be seen in Table 4, the highest contributors to the decay heat at 23.2 years, ^{90}Y and ^{137m}Ba, have relatively small uncertainty, compared to the minor contributors. The small uncertainties of ^{90}Y and ^{137m}Ba is probably because the uncertainties of fission yield and decay data are not considered. Although ^{238}Pu and ^{244}Cm have large uncertainties, their contribution to the decay heat is relatively small. This trend is like those reported for the BWR spent fuel assembly in the reference [11].

When the nuclear data is perturbed, the mean assembly decay heat is 416.96 W, which is different from the base value by −0.029%. The mean decay heat when modeling parameters are perturbed is 417.48 W with a difference of 0.096% from the base value. In both cases, the average values are almost the same as the reference value, indicating that the uncertainty distribution which we have assumed is enough. The base value is the single calculation result using unperturbed nuclear data and modeling parameters. As can be seen in Table 3, the uncertainty due to nuclear data is less than the measurement uncertainty and modeling parameter induced uncertainty, whereas the modeling parameter induced uncertainty and the overall uncertainty are larger than the measurement uncertainty. The overall uncertainty in Table 3 is the quadratic sum of the two different uncertainty sources (nuclear data and modeling parameters) with the assumption of no correlation. Please note that the nuclear data uncertainty excludes the effect due to fission yields and decay data. The result in Table 3 is an example of best estimate plus uncertainty, showing the calculation-experiment comparison together with the uncertainties due to the simulation data (nuclear data, fuel design and irradiation history information) and uncertainty of measurement.

Further analysis of the modeling parameter uncertainties was pursued by fitting each model response from STREAM to a multivariate linear regression using the uncertain input parameters as independent variables. The regression coefficients obtained are then used as sensitivity coefficients. The response relative sensitivities are outlined in Table 5 and has been calculated as the percent change in the response caused by one sigma change in the uncertain parameter value. The relative sensitivities for the specific powers have been lumped into a single specific power effect. In Table 5, the ^{235}U enrichment shows a much larger sensitivity contribution to the neutron source compared to the other response parameters (activity, decay heat, gamma source). The is because ^{235}U is the dominant source of fission in a PWR at the start of irradiation where it accounts for over 90% of all the fission process. After 30 GWd/tU, ^{235}U amount decreases due to burnup and ^{239}Pu becomes the dominant source. For the activity, decay heat and gamma source, the greatest impact is caused by uncertainty in the fuel pellet radius and specific power, followed by the fuel density and moderator temperature. Moreover, the neutron source is mostly affected by the specific power and moderator temperature uncertainties, followed by the fuel pellet radius and fuel density. The burnup at discharge is largely impacted by uncertainty in the specific power. On the other hand, the enrichment, clad outer radius, fuel temperature and boron concentration have negligible impact on the integral source terms. However, these parameters with negligible impact on the integral source terms could affect the nuclide number densities. The rest of this section contains discussion of the UQ workflow and results based on the surrogate model. Then followed by the analysis of UQ results due to modeling parameters and stochastic sampling of nuclear data.

4.1. Uncertainty quantification due to modeling parameters using surrogate models

The results of the PCE, GSA, building the surrogate model and forward UQ due to modeling parameters uncertainties are presented in this section. The workflow is stated as follows:

1) Identify the input parameters and their associated uncertainties as shown in Table 1. The surrogate model is only based on the assembly model parameters, with no consideration for nuclear data.
2) By LHS, generate 100, 300 and 1000 samples with all the input parameters simultaneously perturbed. These represent three sets of input parameters.
3) Perform STREAM calculations on the three different sets of input parameters generated in step 2. Each STREAM run takes about 6 min with a single core on a desktop computer. The input and output data represents the design of experiment.
4) Use results from the first set (of 100 simulations) to build the PCE based surrogate model. For our 11-dimensional input parameter problem, at least 78 model evaluations are required to calculate the coefficients by linear regression method for second order PCE. First and third order PCE require at least 12 and 364 STREAM calculations, respectively.
5) Use the simulation results from the second set (of 300 samples, not used to build the model) to validate the surrogate model, in order to avoid overfitting.
6) Use the surrogate model to evaluate the model responses for third set *i.e.*, 1000 samples.
7) Perform required statistics and GSA on the STREAM and surrogate model evaluations.

Table 4
Calculation results of major decay heat contributors at 23.2 years (%).

Nuclide	Number density (g)	Decay heat (W)	Nuclear data uncertainty (%)	Modeling parameters uncertainty (%)
^{238}Pu	8.93E+01	50.67	2.97	4.02
^{241}Am	4.39E+02	49.94	1.37	3.75
^{244}Cm	8.32E+00	23.57	9.34	6.47
^{90}Y	3.58E-02	107.86	0.17	1.31
^{137m}Ba	5.21E-05	110.08	0.04	1.46

Table 5
Response relative sensitivities at 23 years of cooling.

Parameter	Activity	Decay heat	Neutron source	Gamma source	Burnup[a]
Fuel density	0.44	0.49	0.77	0.40	<0.01
^{235}U enrichment	0.04	−0.03	−0.95	0.07	<0.01
Pellet radius	1.16	1.25	1.77	1.06	<0.01
Fuel temperature	0.05	0.05	0.06	−0.01	<0.01
Clad outer radius	<0.01	<0.01	<0.01	<0.01	<0.01
Specific power	0.78	1.03	3.60	0.76	0.84
Mod Temp	0.41	0.79	3.67	−0.09	<0.01
Boron Conc.	0.01	0.02	0.08	<0.01	<0.01

[a] Results correspond to discharge.

Validation results of the surrogate model are presented in Fig. 2 − 3, comparing the PDFs and model responses with those of STREAM. Fig. 3 shows STREAM results plotted against the surrogate model predictions of the 300 and 1000 samples. A linear fit is included in the plots to capture the linear relationship and good agreement between STREAM results and the surrogate predictions. The good agreement in those figures indicates that the surrogate can accurately map the input space into the model response. The relative validation error of the surrogate is shown in Table 6 for the first order surrogate. This has been evaluated according to Eq. (15) where $\mu_{Y_{Val}}$ is the sample mean of the validation set response. [ξ_{Val}, $y_{Val} = Y(\xi_{Val})$] represent the inputs and outputs of the validation set. In Table 6, the relative validation error of gamma source at 23 years is smaller than at discharge. This is because the surrogate gamma source shows better agreement with STREAM at 23 years than at discharge. For the activity, decay heat and neutron source, the relative validation error at 23 years is larger than at discharge because the surrogate results show better agreement with STREAM at discharge than at 23 years. Although not shown in this report, this explanation is established by the relative differences between STREAM/surrogate at discharge and 23 years. Notwithstanding, the overall STREAM/surrogate agreement is good. Later in this section, the error associated with the surrogate predictions is commented upon to establish its reliability and accuracy. The surrogate model can then be applied to large number of samples at a very cheap computational cost. The computational time required for STREAM to run 1000 cases would be about 6000 min (100 h or 4 days) with single core on a desktop computer. The surrogate model evaluates the model response in about 3 s, significantly reducing the computational burden by orders of magnitude.

$$\varepsilon_{Val} = \frac{N-1}{N}\left[\frac{\sum_{i=1}^{N}\left(Y\left(\xi_{Val}^{(i)}\right) - Y^{PCE}\left(\xi_{Val}^{(i)}\right)\right)^2}{\sum_{i=1}^{N}\left(Y\left(\xi_{Val}^{(i)}\right) - \mu_{Y_{Val}}\right)^2}\right] \tag{15}$$

$$\mu_{Y_{Val}} = \frac{1}{N}\Sigma_{i=1}^{N} Y\left(\xi_{Val}^{(i)}\right) \tag{16}$$

Fig. 4 shows the uncertainties (calculated as relative standard deviation (RSD)) of the SNF characteristics at discharge and after 23.2 years due to modeling parameter uncertainties. It should be noted that the nuclide number density uncertainties in Fig. 4 are not obtained from the surrogate models, they come from the 100 STREAM calculations previously mentioned at the beginning of this section. The neutron source shows a large uncertainty of almost 6% at 23 years. This is followed by an uncertainty of about 2%, 1.6%, 1.4%, 0.8% and 0.5% in the decay heat, activity, gamma source, burnup and effective multiplication factor, respectively, at 23 years. High uncertainty of neutron source is caused by ^{244}Cm (half-life 18.1 years), a dominant neutron source in the first few decades of cooling. At 23 years of cooling, ^{244}Cm accounts for 94.1% of the total neutron source.

The uncertainty of STREAM is compared in Table 7 as a function of number of samples. STREAM uncertainties come from the direct statistics of the results. The results produced by 100 samples show some observable difference compared to 300 and 1000 samples. This difference is caused by convergence issues associated with stochastic sampling requiring large number of repeated runs to obtain converged results. Due to the finite size of the sample considered, statistical errors/statistical fluctuations are present in the results. The standard error of the mean/standard deviation decreases as the sample size is increased until convergence is reached. The PCE based surrogate results are compared to those of STREAM with 1000 samples in Table 8. The mean and RSD of the SNF responses are presented in this table at 23 years of cooling. Please note that the surrogate used in Table 8 is built with first order PCE which requires only 12 simulation results. Moreover, the surrogate results in Table 8 are obtained by applying the first order PCE surrogate to predict the model response of 1000 samples, from which the mean and standard deviation are calculated. The burnup and k-eff results in Tables 7–10 are at discharge and the remaining results are at 23 years of cooling. As can be seen in Table 8, the surrogate results match well with those of STREAM. In further analysis, second and third expansion order surrogates are built and applied to different number of input samples (300, 1000) to predict the model response from which the corresponding uncertainties are calculated. Comparing these results to STREAM, we observe that the first order surrogate is enough for the assembly considered, despite using lower number of calculations for its construction. It is important to mention that the computation time for the first, second or third order surrogate is of the order of few seconds.

The Sobol' sensitivity indices are presented in Fig. 5 showing the total and first order effects at 23 years. The Sobol' indices indicate the main sources of uncertainties and the less important uncertain parameters *i.e.*, the ones that can be excluded from the analysis as they are almost zero. The Sobol' indices for the specific powers have been lumped into a single specific power effect. Fig. 5 shows that the fuel radius, specific power and moderator temperature provides the most important source of uncertainty. The fuel density and the clad radius have contributions to a lesser extent. However, the enrichment, fuel temperature and boron concentration have negligible contributions to the uncertainty of the integral source terms. Further UQ studies on our test problem may exclude these parameters having negligible contributions by using their nominal values. This would then be an example of surrogate model and GSA application in dimensionality reduction, also known as reduced order modeling. The comparison of total and first order Sobol' indices can indicate if interactions between the input parameters have some observable effect on the variance of the output. As shown in Fig. 5, the total and first order Sobol'

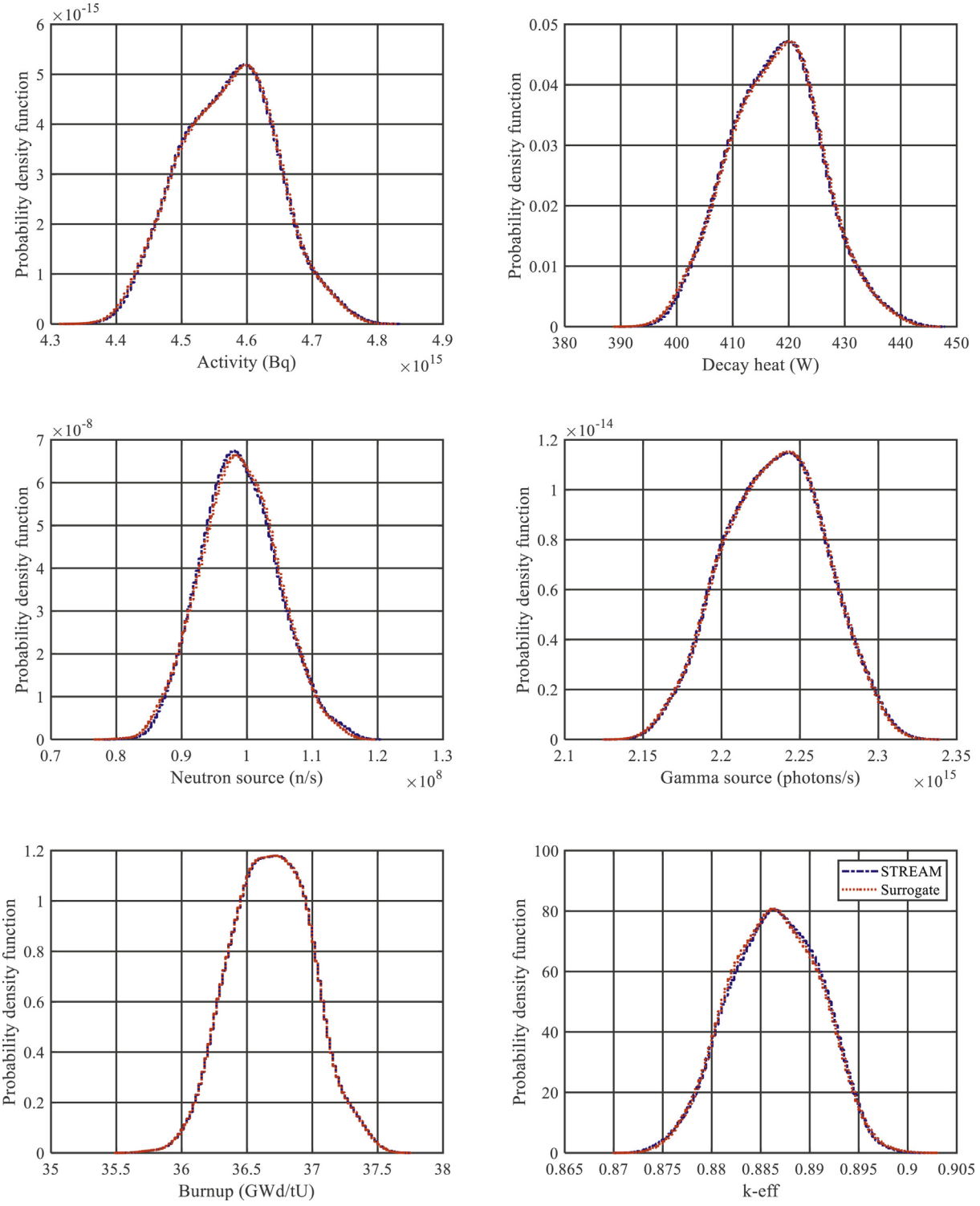

Fig. 2. Comparison of response PDFs at 23 years from 1000 runs.

indices are almost the same because the expected contributions of the high order interactions between the uncertain input parameters to the output variance are small. The input correlations are not considered in the calculations as noted in Section 3, though example of such correlations, for example, between the power and fuel/moderator temperature have been reported [28]. However, correlations between the outputs are observed as can be seen in Fig. 6 when analyzing the results at discharge and for the cooling time considered. The trend of the Sobol' indices in Fig. 5 has similarities with the relative sensitivities in Table 5 with some differences in the neutron source. Concerning the observed differences between Fig. 5 and Table 5, it could be due to the linearity assumption used to evaluate the relative sensitivities in Table 5. This is an approximation if the response depends non-linearly on the parameters, whereas Sobol' indices can be applied to nonlinear responses.

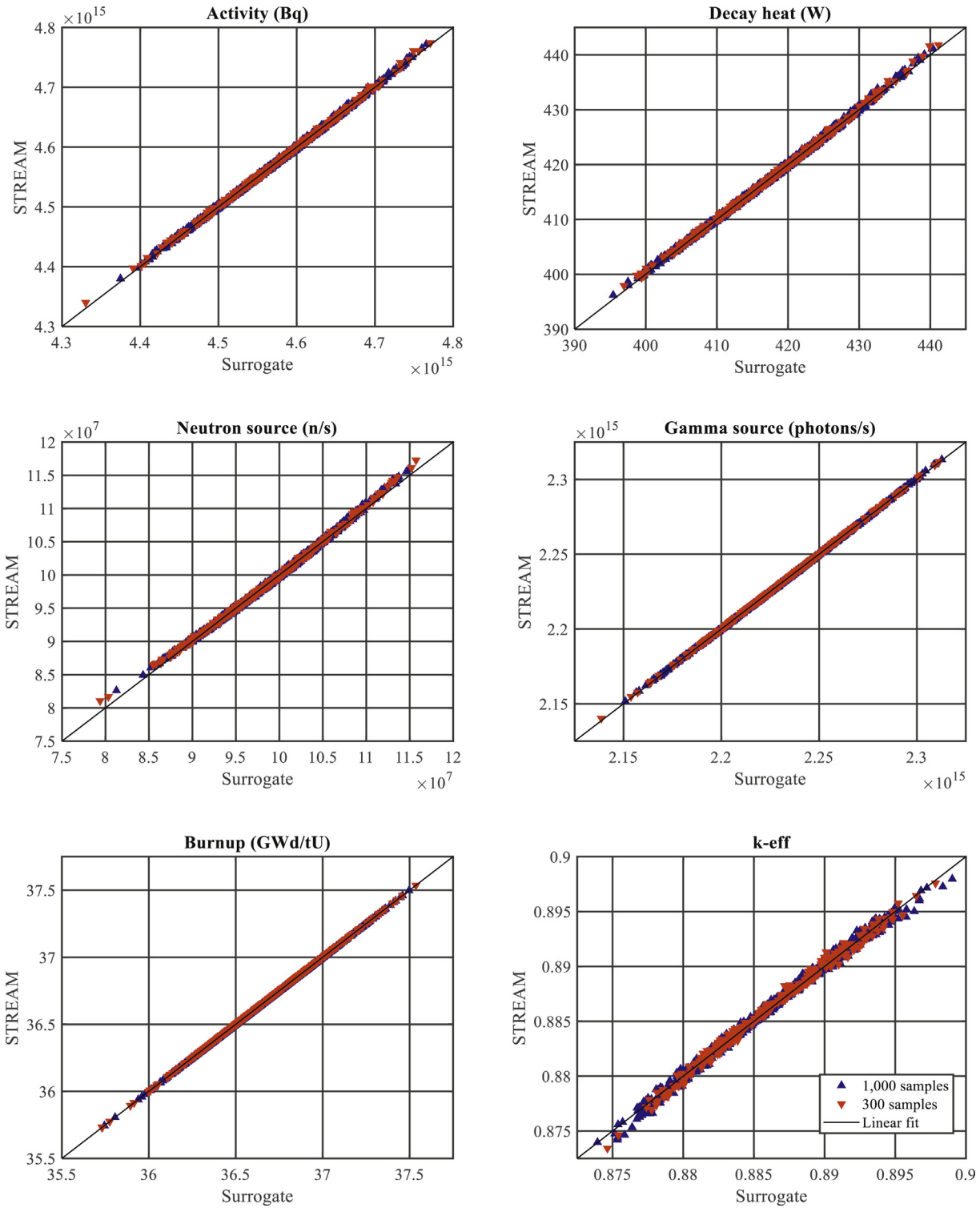

Fig. 3. STREAM results versus surrogate predictions for responses at 23 years.

Table 6
Relative validation error of surrogate model (%).

	Activity	Decay heat	Neutron source	Gamma source	Burnup	k-eff
Discharge	3.39E-02	1.92E-02	2.09E-02	2.67E-02	8.94E-05	6.67E-01
23 years	1.10E-01	1.90E-01	3.12E-01	1.64E-02	-	-

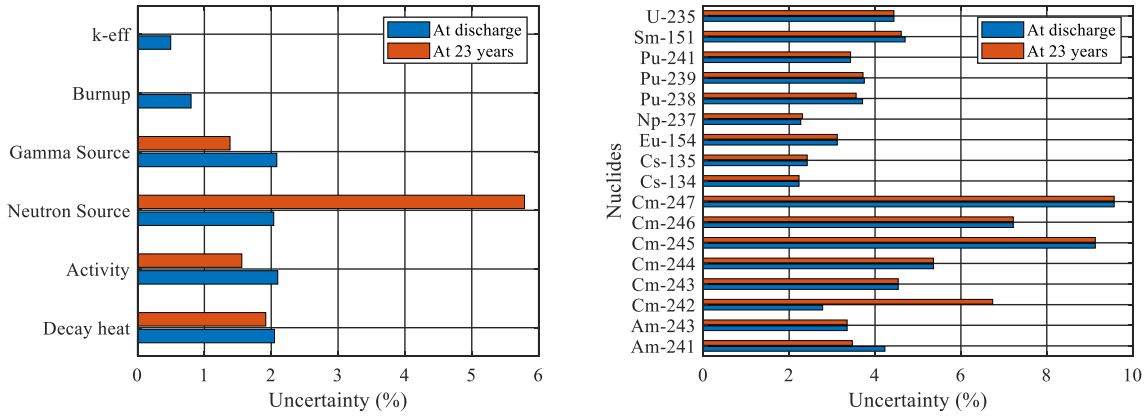

Fig. 4. Uncertainties of SNF characteristics (left) and nuclides densities (right) due to modeling parameters.

Table 7
STREAM response uncertainty at 23 years of cooling (%).

N samples	Activity	Decay heat	Neutron source	Gamma source	Burnup[a]	k-eff[a]
100	1.43	1.73	5.25	1.32	0.86	0.57
300	1.61	2.02	6.32	1.39	0.88	0.50
1000	1.55	1.91	5.80	1.38	0.80	0.50

[a] See footnote of Table 5.

Table 8
Response moments at 23 years of cooling.

Response	Mean		RSD (%)	
	STREAM	Surrogate	STREAM	Surrogate
Activity (Bq)	4.5697E+15	4.5695E+15	1.55	1.56
Decay heat (W)	4.1747E+02	4.1745E+02	1.91	1.92
Neutron source (n/s)	9.8740E+07	9.8718E+07	5.80	5.79
Gamma source (photons/s)	2.2331E+15	2.2331E+15	1.38	1.38
Burnup[a] (GWd/tU)	3.6676E+01	3.6676E+01	0.80	0.80
k-eff[a] (−)	8.8627E-01	8.8624E-01	0.50	0.50

[a] See footnote of Table 5.

For the surrogate point-wise predictions, the error due to the finite size of input data is estimated by bootstrap method [29]. One hundred sample sets are drawn from the first set of input data by resampling with substitution to create bootstrap replications. Each replication has the same size as the first set of input data and is used to calculate a PCE. This produces a set of 100 different surrogate models with coefficients and responses. The sets of responses are then used to calculate the standard deviation of the surrogate point-wise predictions due to the finite size of input data. The maximum relative standard deviation of the first order surrogate point-wise predictions is reported in Table 9. Moreover, the sets of PCE coefficients from the bootstrap replications have also been used to estimate the standard deviation of the surrogate-predicted mean and standard deviation shown in Table 8. These results are presented in Table 10. These tables show that the errors associated with the surrogate point-wise predictions, mean and standard deviations are small as we assess the accuracy of the surrogate model. The error analysis of the surrogate predictions can be used to obtain an interval in which the true value exist at a given confidence level.

4.2. Uncertainty quantification due to nuclear data

To bring the results into perspective, the impact of nuclear data uncertainties in PWR UO_2 SNF is provided based on the previous discussions in Section 3.1.1. The test case assembly used in this work is previously described in Section 2. Three hundred (300) STREAM calculations are performed using the perturbed cross section and RI libraries, and the SNF characteristics are statistically processed to

Table 9
Maximum RSD of surrogate point-wise predictions at 23 years.

	Activity	Decay heat	Neutron source	Gamma source	Burnup[a]	k-eff[a]
RSD (%)	3.14E-02	4.91E-02	1.86E-02	8.79E-03	3.00E-04	2.15E-02

[a] See footnote of Table 5.

Table 10
Error of surrogate model mean and standard deviation at 23 years (%).

	Activity	Decay heat	Neutron source	Gamma source	Burnup[a]	k-eff[a]
RSD of mean	4.83E-03	7.06E-03	2.74E-02	1.58E-03	7.95E-05	4.07E-03
RSD of σ	4.91E-01	6.56E-01	8.94E-01	1.47E-01	9.89E-03	8.64E-01

[a] See footnote of Table 5.

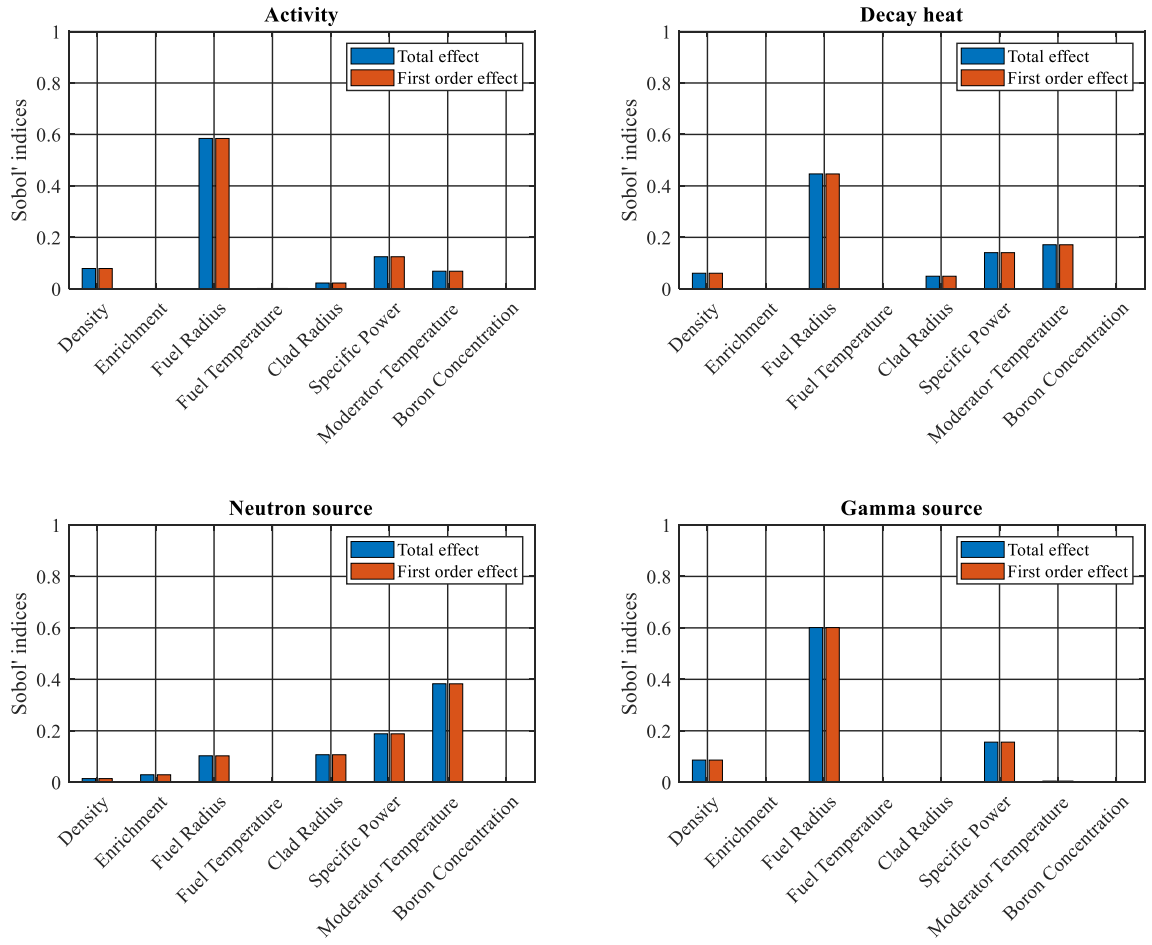

Fig. 5. Sobol' indices (total and first order effects) for uncertain input parameters at 23 years.

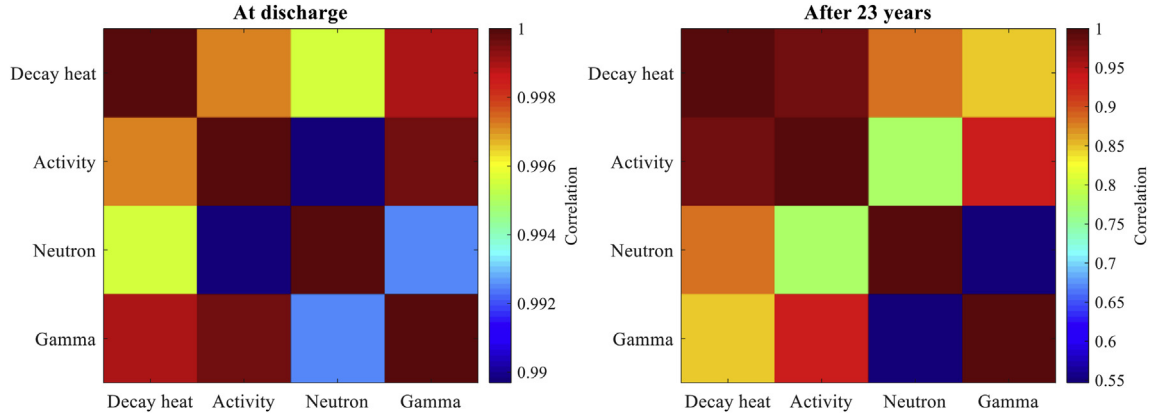

Fig. 6. Correlation matrix of source terms for the 15 × 15 fuel assembly.

obtain the uncertainties. During burnup, the results of nuclear data induced uncertainties of the nuclide number densities and source terms are presented in Fig. 7a – 12a. The discussion of the results contained in those figures will be presented in this section. Later in this section, the results of nuclear data induced uncertainties of the nuclide number densities and source terms during cooling time will be analyzed.

Fig. 7a presents the uncertainties of uranium number densities. The uncertainties of ^{234,235}U increase with burnup as their number densities decrease. At discharge burnup of 36.7 GWd/tU, the uncertainty in ^{234}U is less than 0.4%, while that of ^{235}U is about 1.2%. Uncertainty of ^{236}U is almost constant during burnup at a value of 1.2%, whereas ^{238}U has nearly zero uncertainty because it does not change much from its initial amount during irradiation. Uncertainties of plutonium isotopes are shown in Fig. 8a. ^{238}Pu has high uncertainty at low burnup when the amount is small. ^{238,239,240,241,242}Pu have uncertainties between 1.5% and 3.5% at discharge. The uncertainties in the minor actinides are illustrated in

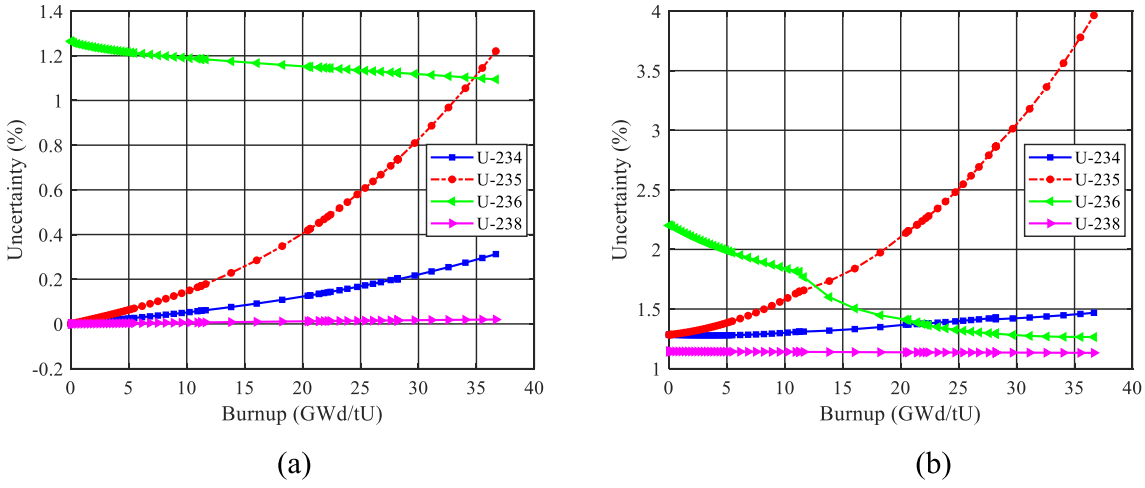

Fig. 7. Uncertainty of uranium number densities against burnup due to (a) nuclear data and (b) modeling parameters.

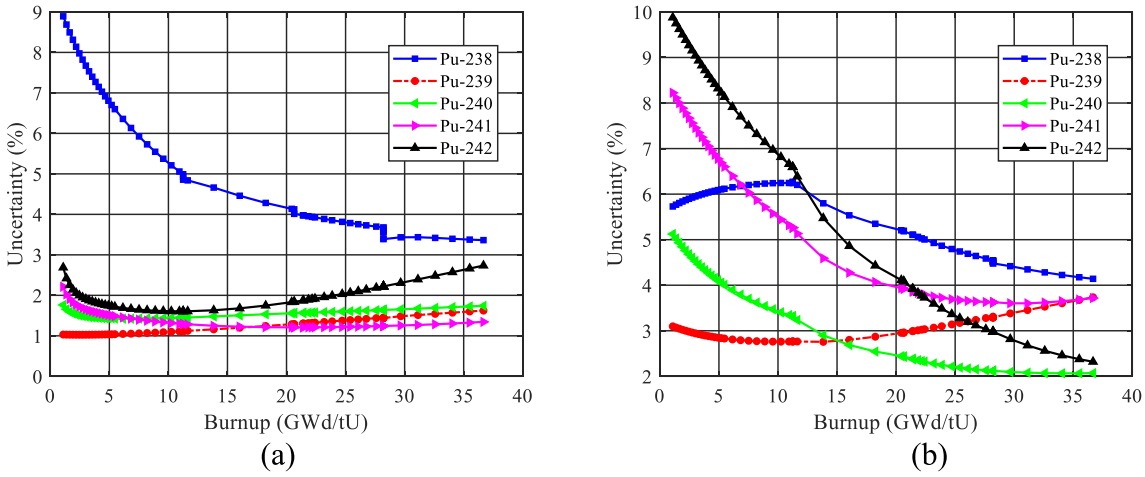

Fig. 8. Uncertainty of plutonium number densities against burnup due to (a) nuclear data and (b) modeling parameters.

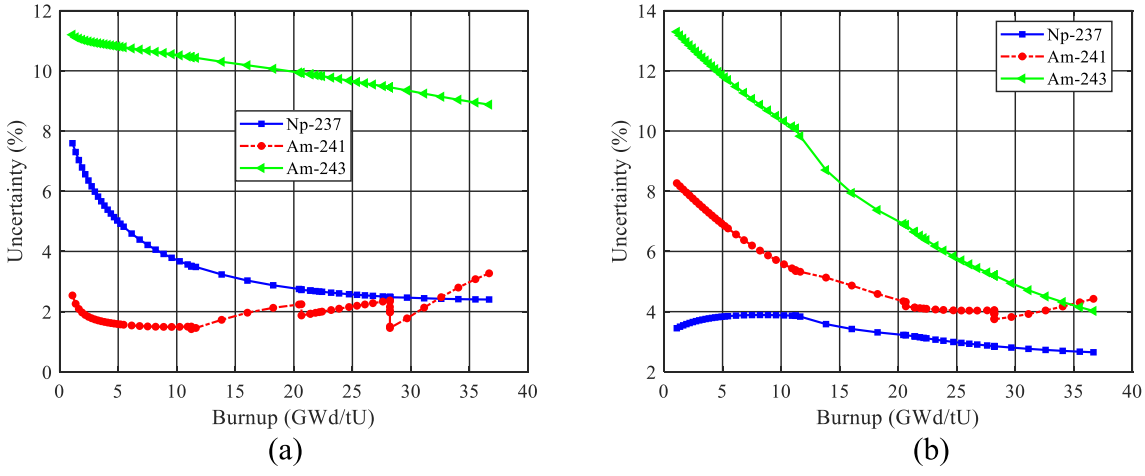

Fig. 9. Uncertainty of minor actinides number densities against burnup due to (a) nuclear data and (b) modeling parameters.

Figs. 9a and 10a. These are higher than those of the major actinides. Uncertainties of ^{243}Am and ^{244,245}Cm slowly decrease during burnup and remains high at values between 8% and 13% at discharge. The increasing trend of the concentration of minor actinides during burnup is responsible for their decreasing uncertainties. Uncertainty of ^{241}Am varies between 2% and 3% from 2

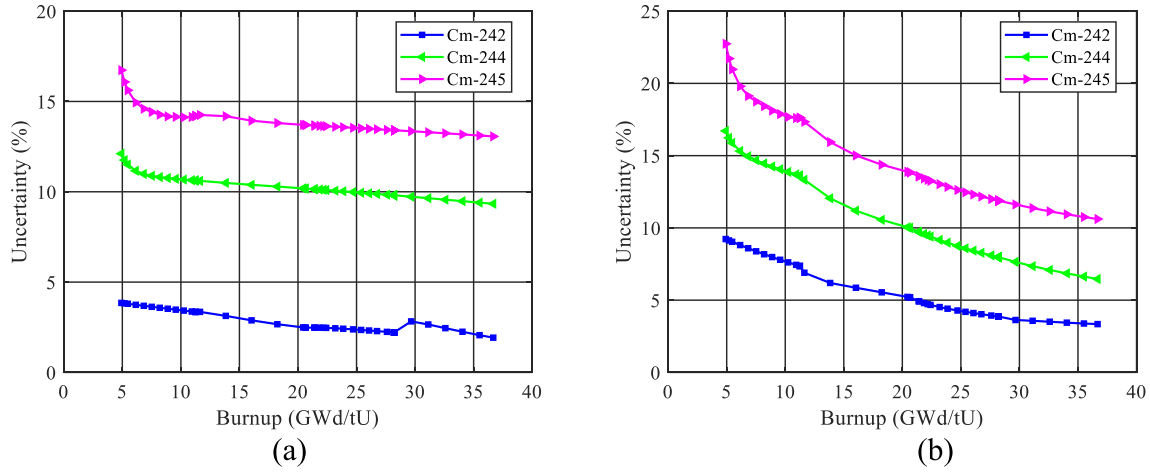

Fig. 10. Uncertainty of curium number densities against burnup due to (a) nuclear data and (b) modeling parameters.

to 37 GWd/tU burnup. The drop off in ^{241}Am uncertainty around 21 and 28 GWd/tU is caused by the inter-cycle cooling times modeled in the irradiation history. As stated in Table 2, the assembly was irradiated in the reactor during four cycles. During irradiation, there were three down times which occurred after burnups of 11, 21 and 28 GWd/tU, respectively. For this reason, some uncertainties in Figs. 7–12 may experience sudden increase/decrease around these burnup values. The use of constant power depletion will eliminate the drop offs. The constant power being derived from the final burnup divided by the number of operating days. However, this approach will introduce another modeling uncertainty *i.e.*, uncertainty in the power history, which will bias the number densities. And quite several nuclides are much sensitive to the power history, a good example of which is ^{241}Am [3]. Uncertainties in some fission products are shown in Fig. 11a. Uncertainties of ^{135}Cs and ^{154}Eu shows some increasing trend but remain very low ~0.5% at end of burnup. ^{137}Cs and ^{144}Ce have nearly zero uncertainty during depletion. However, ^{134}Cs has high uncertainty between 4% and 5% throughout burnup. It is important to note that the nuclear data uncertainties do not include the effect of uncertainties due to fission yields and decay data. Fig. 12a contains the uncertainties of radiation source terms during irradiation. The activity and gamma source have decreasing uncertainties whereas the decay heat and neutron source show increasing uncertainties with burnup. However, these uncertainties are low and remain below 0.6% after burnup.

Next we analyze the results of nuclear data induced uncertainties of the nuclide number densities and source terms during cooling time. During cooling, the uncertainties of the nuclide number densities and source terms due to nuclear data uncertainties are presented in Fig. 13a – 18a. The uncertainties of uranium isotopes as a function of cooling time are presented in Fig. 13a. There is a steady increase in ^{234}U uncertainty between 10 and 500 years of cooling. Although this uncertainty remains less than 2% up until 10,000 years. The uncertainties of ^{235,236,238}U are constant after discharge as their number densities do not change due to their very long half-lives. The uncertainties for these major actinides are 1.2%, 1.1%, and 0.0%, respectively. Uncertainties of plutonium isotopes during cooling are shown in Fig. 14a. For ^{238,239,240,242}Pu, the uncertainties nearly do not change up to 10,000 years and stands between 2% and 3%. A sharp increase in ^{241}Pu uncertainty is noted after 200 years, rising to about 13% and remaining constant from 500 to 10,000 years after discharge. We refined the cooling time steps between 200 and 500 years to examine the cause of the abrupt increase in ^{241}Pu uncertainty. After the refinement, we observed the same behavior between 200 and 500 years. The variation of ^{241}Pu number density during cooling shows that the sharp increase in ^{241}Pu uncertainty is due to the

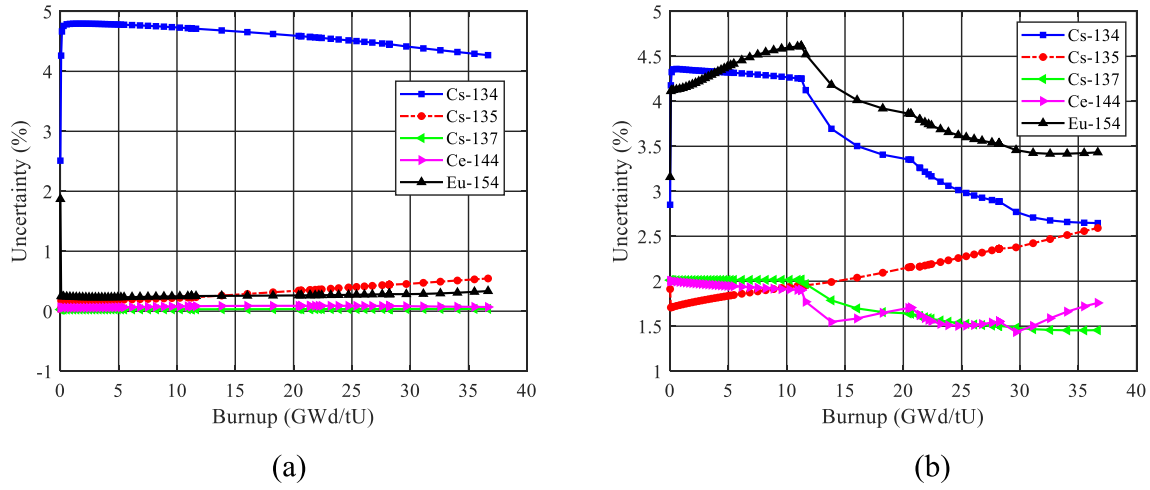

Fig. 11. Uncertainty of fission products number densities against burnup due to (a) nuclear data and (b) modeling parameters.

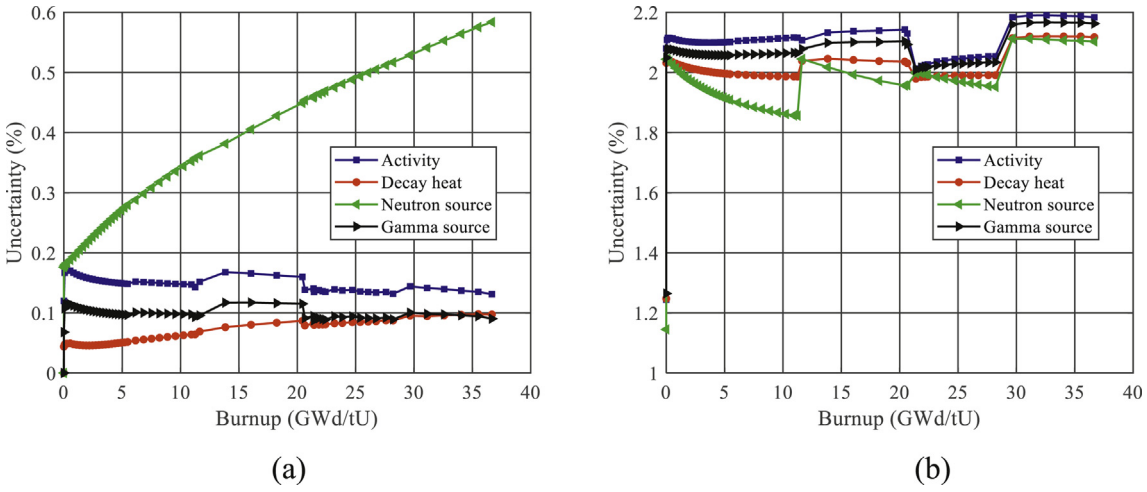

Fig. 12. Uncertainty of SNF characteristics against burnup due to (a) nuclear data and (b) modeling parameters.

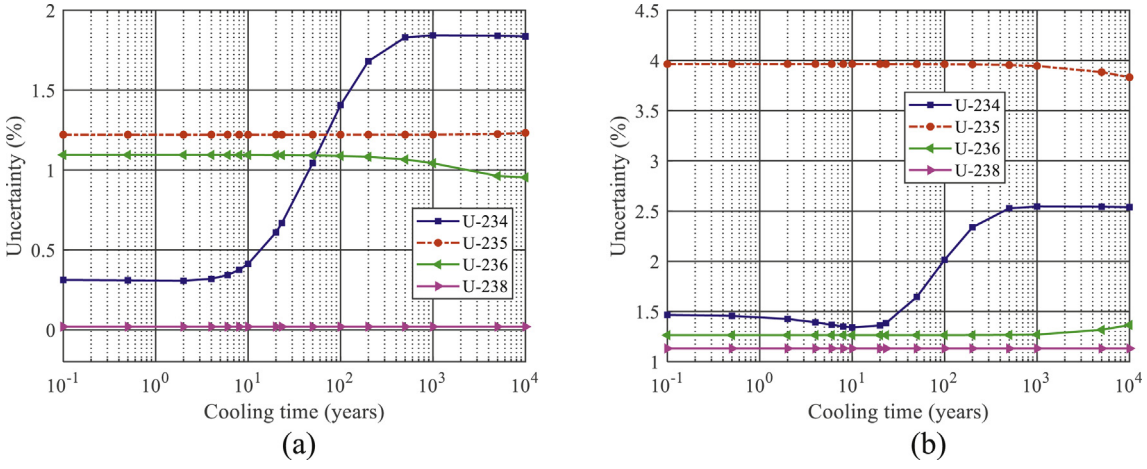

Fig. 13. Uncertainty of uranium number densities against cooling time due to (a) nuclear data and (b) modeling parameters.

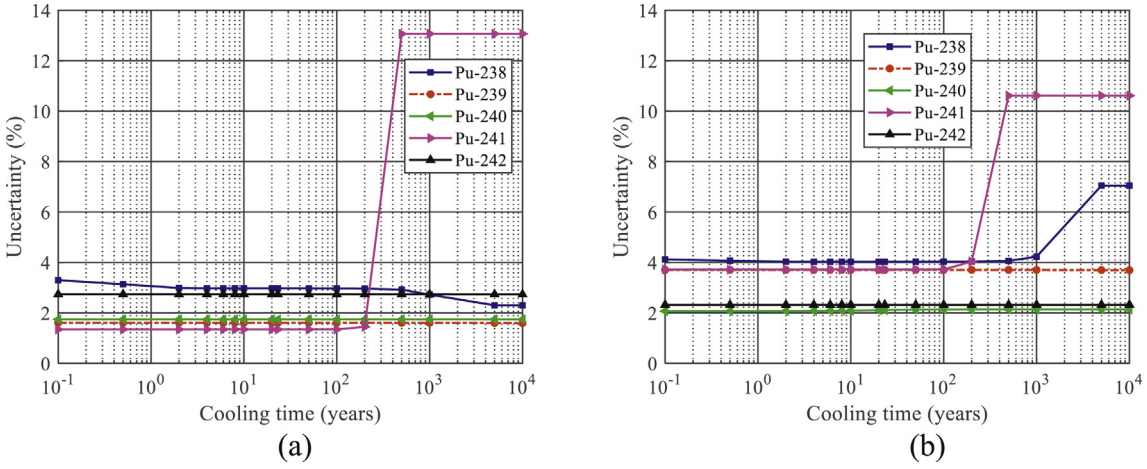

Fig. 14. Uncertainty of plutonium number densities against cooling time due to (a) nuclear data and (b) modeling parameters.

decrease of its number density. From 500 to 10,000 years, the uncertainty is constant because ^{241}Pu number density remains almost unchanged. The uncertainties in the minor actinides are illustrated in Figs. 15a and 16a as a function of cooling time. Uncertainties of ^{243}Am and ^{244,245}Cm are constant and remain high at 9%, 9% and 13%, respectively. Uncertainty of ^{241}Am decreases from 3% at 0.1 year to about 1.5% at 10 years, and remains constant up to 1000 years, and then rose to 13% at 10,000 years. Uncertainty of ^{237}Np

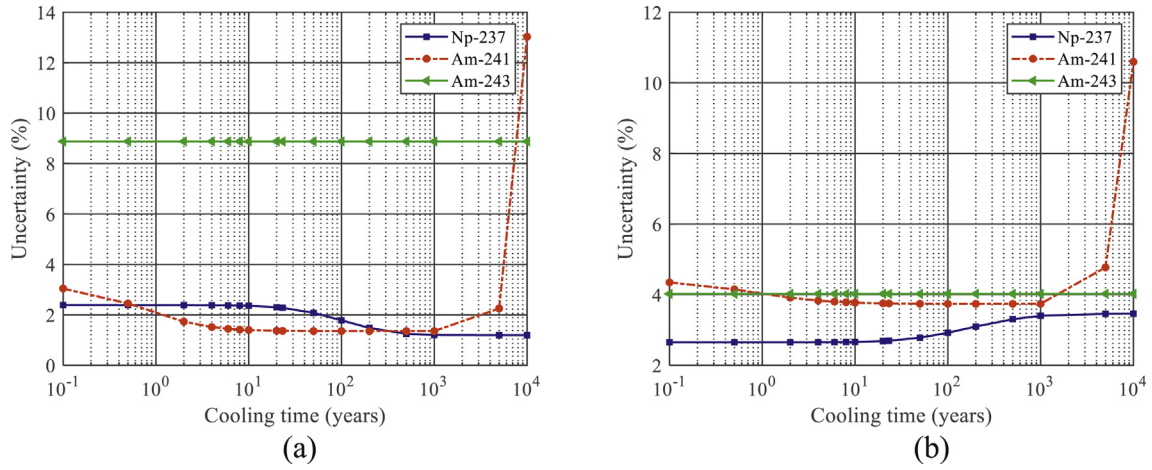

Fig. 15. Uncertainty of minor actinides number densities against cooling time due to (a) nuclear data and (b) modeling parameters.

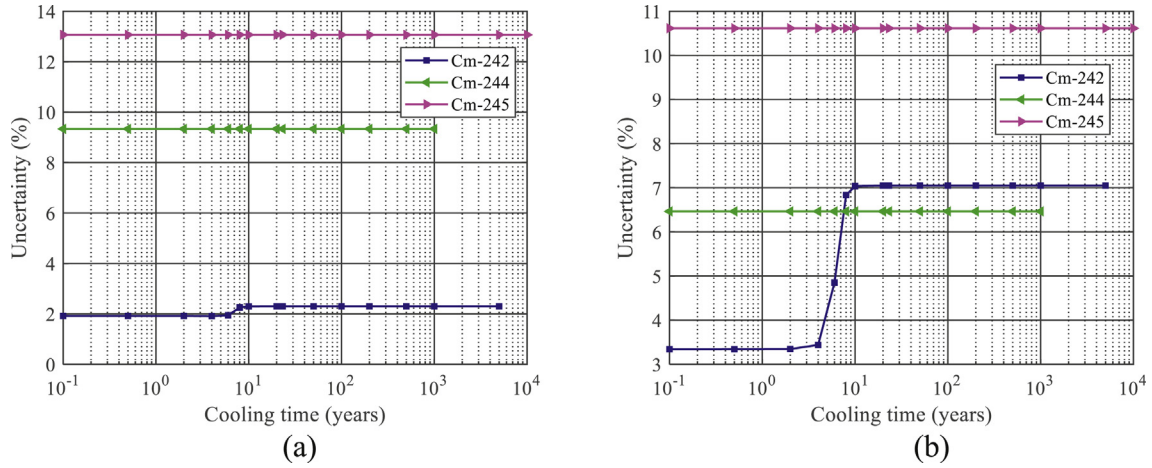

Fig. 16. Uncertainty of curium number densities against cooling time due to (a) nuclear data and (b) modeling parameters.

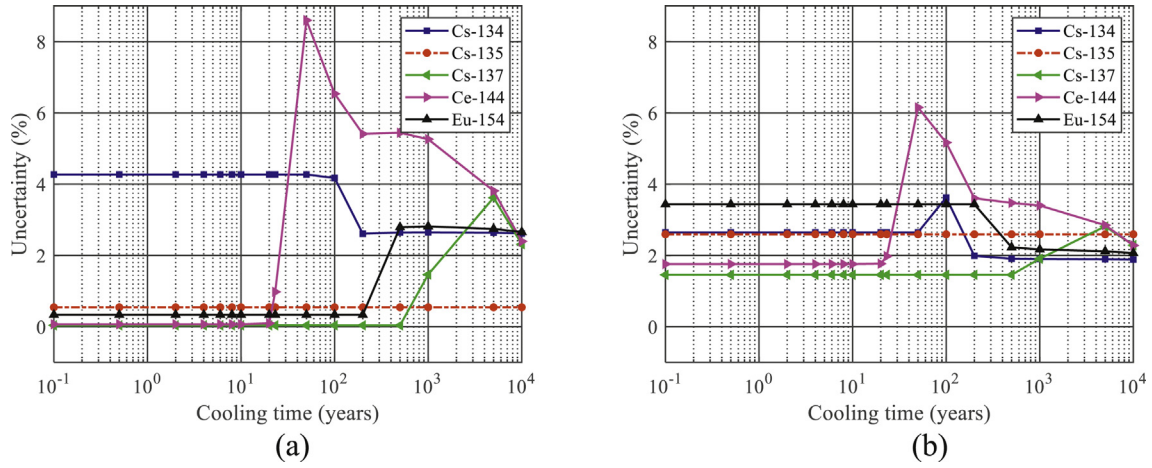

Fig. 17. Uncertainty of fission products number densities against cooling time due to (a) nuclear data and (b) modeling parameters.

stands at about 2.5% from 0.1 to 20 years and drops to 1% between 200 and 10,000 years.

Fig. 17a shows some fission product uncertainties during cooling. ^{134}Cs uncertainty stands at 4% after discharge until 100 years and decreases to about 2.5% afterwards. ^{135}Cs uncertainty remains constant at 0.5% due to its long half-life of 2.3 million years. ^{137}Cs uncertainty is 0% until 500 years, then it rises to about 4% at 5000 years and decreases to about 2.5% at 10,000 years. ^{144}Ce has an

uncertainty of 0% until about 20 years, then the uncertainty increases to 8.5% at 50 years, followed by a decrease to 2.5% at 10,000 years. ^{154}Eu shows constant trend of uncertainty below 0.5% until 200 years, and then the uncertainty increases to about 3% at 500 years. This increase in uncertainty of ^{137}Cs, ^{144}Ce, and ^{154}Eu can be attributed to the decrease of their number densities. ^{134}Cs, ^{154}Eu, and ^{144}Ce (and its decay product) are important to SNF decay heat in the first 10 years of cooling. ^{137}Cs and its decay product is important to decay heat after 20 years as can be seen in Table 4 where ^{137}Cs and its decay product ^{137m}Ba are among the major decay heat contributors at 23 years.

The uncertainties of radiation source terms during cooling are contained in Fig. 18a. The activity, decay heat and gamma source have slightly increasing uncertainties which is within 1% up until 100 years. Moreover, the uncertainties of these three radiation source terms lie within 1.5% from 100 to 10,000 years, except for the gamma source uncertainty which rises to about 4% around 5000–10,000 years. For the activity, decay heat and gamma source, the maximum uncertainty occurs at long cooling time. For the decay heat, this trend here is like those observed in previously analyzed PWR and BWR spent fuel assemblies [6,11]. The fission products are the major contributor to these source terms at cooling times up to 100 years. Many of the fission products decay out at longer cooling times beyond 100 years and the actinides become the major contributors. The neutron source uncertainty is however much larger, increasing from 4% at 0.1 year to a maximum of 9% at around 10 years, and then followed by a decrease to between 4% and 6%. Fig. 18a shows that the maximum neutron source uncertainty occurs at short cooling time around 10 years where the total neutron source is dominated by ^{244}Cm (96.6%). In general, the neutron source uncertainty at less than 100 years is mostly dominated by the uncertainties of the major neutron source ^{244}Cm.

4.3. Discussion of nuclear data and modeling parameter induced uncertainties

The evolution of the modeling parameter induced uncertainties during burnup and after discharge for the PWR assembly described in Section 2 are presented in Figs. 7b–18b. The results in these figures are not obtained from the surrogate model discussed in Sections 3.2 and 4.1. Rather, three hundred (300) STREAM SNF calculations are performed with all the modeling parameters listed in Table 1 perturbed simultaneously. The modeling parameter induced uncertainties are extracted from the statistical processing of the 300 STREAM results. The modeling parameter induced uncertainties are first discussed in this section, then the comparison between the uncertainties caused by nuclear data and the modeling parameters is discussed.

During burnup, the uncertainties of the nuclide number densities and source terms, due to modeling parameters uncertainties, are shown in Figs. 7b–12b. Fig. 7b shows the uncertainties of uranium isotopes. The uncertainty of ^{234}U slightly increases with burnup and reaches 1.5% at 36.7 GWd/tU. ^{234}U is very sensitive to uncertainties in its initial concentration due to its very small initial amount. Between 0 and 36.7 GWd/tU burnup, ^{235}U uncertainty rises from 1.25% to 4%, while the uncertainty of ^{236}U decreases from 2.3% to 1.3%. ^{238}U has constant uncertainty of about 1.2% throughout the irradiation. The uncertainties of uranium isotopes are likely to have been affected by uncertainty in the fuel enrichment. Plutonium isotopes ^{238,240,241,242}Pu show decreasing uncertainty in Fig. 8b with values of 4%, 2%, 3.5%, and 2.5%, respectively, at the end of burnup. ^{239}Pu is very sensitive to the neutron spectrum and its uncertainty mostly likely is due to uncertainties in the clad outer radius and fuel radius which can affect the moderation ratio. The minor actinides uncertainties can be seen in Figs. 9b and 10b. These display a decreasing trend. Although these uncertainties remain high at the end of burnup, except for ^{237}Np. ^{241}Am is sensitive to uncertainties in the power history. The curium isotopes are much more sensitive to uncertainties in the burnup at the end of irradiation, because they are at the end of the burnup chain. Uncertainty in the burnup due to modeling parameters is observed to be less than about 1% at the end of irradiation. Uncertainties of selected fission products are shown in Fig. 11b. Uncertainties of ^{134}Cs and ^{154}Eu shows some decreasing trend from about 4.5% at 12 GWd/tU to 2.5% and 3.5%, respectively, at the end of burnup. ^{137}Cs and ^{144}Ce have nearly constant uncertainty of 2% up until 12 GWd/tU which then decreases to about 1.5% towards the end of irradiation. However, ^{135}Cs has a slightly increasing trend in uncertainty with a value of 2.5% at 36.7 GWd/tU. The fission products ^{134}Cs and ^{144}Ce are also sensitive to the power history.

The comparison between the uncertainties caused by nuclear data and the modeling parameters is discussed. Figs. 12 and 18 show that during burnup and cooling, the uncertainties in activity, decay heat and gamma source are dominated by uncertainties in the modeling parameters (*i.e.*, fuel design and irradiation history). For the neutron source, the uncertainties during burnup are dominated by fuel design and irradiation history uncertainties whereas during cooling the nuclear data uncertainties dominate.

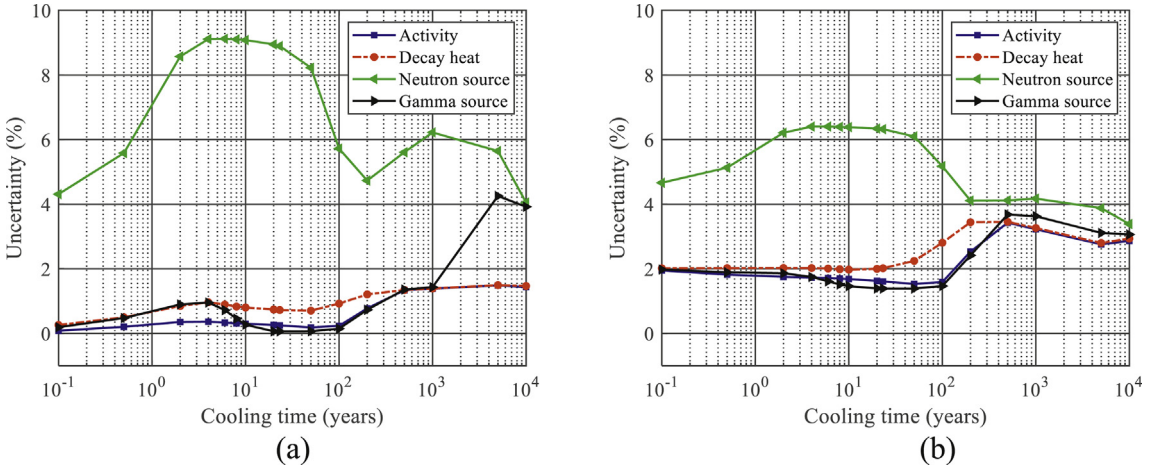

Fig. 18. Uncertainty of SNF characteristics against cooling time due to (a) nuclear data and (b) modeling parameters.

On the number densities, for ^{234,235,236,238}U, ^{241}Am, and ^{239}Pu, the uncertainties due to modeling parameters are larger during burnup and cooling. For ^{237}Np, uncertainties due to nuclear data are larger up to 10 GWd/tU burnup, after which it becomes comparable to those due to modeling parameters. During cooling, uncertainties due to modeling parameters are larger. For ^{243}Am, uncertainties due to modeling parameters are larger up to 10 GWd/tU burnup, then uncertainties due to nuclear data are larger between 10 and 36 GWd/tU burnup. During cooling, uncertainties due to nuclear data are larger by a factor of 2.3. For ^{243,244,245,246,247}Cm, the nuclear data induced uncertainties are larger during cooling. For the fission products, ^{154}Eu shows a larger modeling parameter induced uncertainty during burnup and up to 200 years of cooling. In the case of ^{135}Cs, the modeling parameter induced uncertainties are larger during burnup and cooling. ^{134}Cs shows a larger nuclear data induced uncertainty during burnup and cooling. Modeling parameter induced uncertainties are larger in ^{137}Cs during burnup and up to 1000 years of cooling. For ^{144}Ce, the modeling parameter induced uncertainties are larger during burnup and up to 23 years of cooling. From 50 to 5000 years of cooling, uncertainties due to nuclear data are larger. In general, it can be seen from the results that the uncertainties of SNF due to modeling parameters are non-negligible.

5. Conclusions

Uncertainties are evaluated for a PWR spent fuel assembly characteristics: isotopic compositions, activity, decay heat, neutron and gamma sources. The uncertainties in nuclear data (cross sections and resonance integral parameters) and modeling parameters (fuel design and irradiation history information) are propagated by stochastic sampling. The depletion and source term calculations are conducted with the neutron transport and depletion capabilities of the deterministic code STREAM. The SNF characteristics are evaluated for burnup up to 36.7 GWd/tU and cooling times up to 10,000 years. Surrogate models are also applied to demonstrate SA and UQ of SNF due to modeling parameter uncertainties. PCE based surrogate model and Sobol' indices are employed in an 11-dimensional input parameter problem to analyze the uncertainties and perform GSA. The surrogate model achieves similar accuracy with small number of repeated calculations.

For the assembly, at the time of decay heat measurement, 23.2 years of cooling, the calculated decay heat is significantly impacted by uncertainties in fuel design and irradiation history information (2.0%). The impact of cross section data and RI uncertainties is 0.7%. The overall uncertainty on the calculated decay heat is about 2.1% and it is larger than the experimental uncertainty. The large calculation uncertainty is dominated by the model parameter uncertainty. This could be due to (i) the correlations between the input parameters are not considered; (ii) lack of fuel vendor proprietary information *i*.e., actual manufacturing tolerances are not known for the assembly studied; (iii) large input uncertainties of the model parameters, assumptions of uncertainties and their PDFs; (iv) lack of consideration of fission yield and decay data uncertainties. These limitations will be addressed in the future work. For the nuclear data induced uncertainty, it is observed that the decay heat uncertainty increases with burnup and the maximum decay heat uncertainty occurs at longer cooling times when the actinides become the main contributors. The observed trend of the decay heat uncertainty due to nuclear data as a function of burnup and cooling time is almost identical to that of a PWR and BWR spent fuel assembly analyzed by other authors [6,11].

Though the uncertainties reported here for the assembly considered are large, it may differ for other enrichments, burnup ranges and assembly designs. This study shows a computationally efficient approach for accurately evaluating uncertainties in integral source terms due to modeling parameter uncertainties. It is also shown in this study that the impact of fuel design and irradiation history uncertainty can be important (*e.g.* up to 6% for the neutron source) and that modeling parameters have non-negligible impact on SNF isotopic inventory and radiation source terms. The nuclide number densities, neutron and gamma sources calculated from perturbed nuclear data and modeling parameters will be important in applications where the SNF isotopic inventories and source terms are required such as in SNF cask dose rate analysis, radiation shielding and nuclear safeguards by non-destructive assay techniques, for further uncertainty propagation and quantification studies.

Declaration of competing interest

The authors declare that they have no known competing financial interests or personal relationships that could have appeared to influence the work reported in this paper.

Acknowledgments

This work was supported by the National Research Foundation of Korea (NRF) grant funded by the Korea government (MSIT). (No. NRF-2019M2D2A1A03058371).

References

[1] J. Choe, S. Choi, P. Zhang, J. Park, W. Kim, H.C. Shin, H.S. Lee, J. Jung, D. Lee, Verification and validation of STREAM/RAST-K for PWR analysis, Nucl. Eng. Tech. 51 (2019) 356–368.
[2] N.N.T. Mai, P. Zhang, M. Lemaire, B. Ebiwonjumi, W. Kim, H. Lee, D. Lee, Extension of Monte Carlo code MCS to spent fuel cask shielding analysis, Int. J. Energy Res. (2020), https://doi.org/10.1002/er.5023.
[3] B. Ebiwonjumi, S. Choi, et al., Validation of lattice physics code STREAM for predicting pressurized water reactor spent nuclear fuel isotopic inventory, Ann. Nucl. Energy 120 (2018) 431–449.
[4] B. Ebiwonjumi, S. Choi, et al., Verification and validation of radiation source term capabilities in STREAM, Ann. Nucl. Energy 124 (2019) 80–87.
[5] B.T. Rearden, D.E. Mueller, S.M. Bowman, R.D. Busch, S.J. Emerson, TSUNAMI Primer: A Primer for Sensitivity/Uncertainty Calculations with SCALE, 2009.
[6] M. Williams, G. Ilas, et al., A statistical sampling method for uncertainty analysis with SCALE and XSUSA, Nucl. Technol. 183 (2013) 515–526.
[7] W. Wieselquist, T. Zhu, A. Vasiliev, H. Ferroukhi, PSI methodologies for nuclear data uncertainty propagation with CASMO-5M and MCNPX: results for OECD/NEA UAM benchmark phase I, Sci. Technol. Nucl. Install. (2013), https://doi.org/10.1155/2013/549793.
[8] B. Krzykacz, E. Hofer, M. Kloos, A software system for probabilistic uncertainty and sensitivity analysis of results from computer models, in: Int. Conf. Probabilistic Safety Assessment and Management (PSAM-II), 1994. San Diego, California, March 20-25.
[9] D.A. Rochman, A. Vasilev, et al., Uncertainties for Swiss LWR spent nuclear fuels due to nuclear data, EPJ Nucl. Sci. Tech. 4 (2018) 1–13.
[10] O. Leray, D. Rochmman, P. Grimm, et al., Nuclear data uncertainty propagation on spent fuel nuclide compositions, Ann. Nucl. Energy 94 (2016) 603–611.
[11] G. Ilas, H. Liljenfeldt, Decay heat uncertainty for BWR used fuel due to modeling and nuclear data uncertainties, G. Nucl. Eng. Des. 319 (2017) 176–184.
[12] D. Rochman, A. Vasiliev, H. Ferroukhi, et al., Best estimate plus uncertainty analysis for the ^{244}Cm prediction in spent fuel characterization, in: ANS Best Estimate Plus Uncertainty International Conference (BEPU 2018), 2018. Real Collegio, Lucca, Italy, May 13 – 19.
[13] OECD/NEA, State of the Art Report on Spent Nuclear Fuel Assay Data for Isotopic Validation, Organization for Economic Cooperation and Development, Nuclear Energy Agency, Nuclear Science Committee, Working Party on Nuclear Criticality Safety, 2011. Technical Report NEA/NSC/WPNCS/DOC(2011) 5.
[14] K. Sargsyan, Surrogate models for uncertainty propagation and sensitivity analysis, in: R. Ghanem, D. Higdon, H. Owhadi (Eds.), Handbook of Uncertainty Quantification, Springer International Publishing, 2017, pp. 673–698. Switzerland.
[15] L. Gilli, D. Lathouwers, et al., Uncertainty quantification for criticality problems using non-intrusive and adaptive Polynomial Chaos techniques, Ann. Nucl. Energy 56 (2013) 71–80.
[16] Z. Perkó, D. Lathouwers, et al., Large scale applicability of a fully adaptive non-intrusive spectral projection technique: sensitivity and uncertainty analysis of a transient, Ann. Nucl. Energy 71 (2014) 272–292.

[17] S. Marelli, B. Surety, UQLab: a framework for uncertainty quantification in Matlab, in: 2nd Int. Conf. On Vulnerability, Risk Analysis and Management (ICVRAM2014), 2014. Liverpool, United Kingdom, July 13-16.
[18] SKB, Measurements of Decay Heat in Spent Nuclear Fuel at Swedish Interim Storage Facility, *CLAB*. Svensk Kärnbränslehantering AB (SKB), Swedish Nuclear Fuel and Waste Management Co., 2006, pp. R-05–62.
[19] S. Choi, C. Lee, D. Lee, Resonance treatment using pin-based pointwise energy slowing-down method, J. Comput. Phys. 330 (2017) 134–155.
[20] S. Choi, K. Smith, H.C. Lee, D. Lee, Impact of inflow transport approximation on light water reactor analysis, J. Comput. Phys. 299 (2015) 352–373.
[21] Akio Yamamoto, Kuniharu Kinoshita, Tomoaki Watanabe, Tomohiro Endo, Uncertainty quantification of LWR core characteristics using random sampling method, Nucl. Sci. Eng. 181 (2015) 160–174.
[22] S. Choi, C. Lee, D. Lee, Resonance self-shielding method using resonance interference factor library for practical lattice physics computations of LWRs, J. Nucl. Sci. Technol. 53 (2016) 1142–1154.
[23] S. Choi, H. Lee, S.G. Hong, D. Lee, Resonance self-shielding methodology of new neutron transport code STREAM, J. Nucl. Sci. Technol. 52 (2015) 1133–1150.
[24] S. Marelli, B. Sudret, UQLAB User Manual – Polynomial Chaos Expansions, Chair of Risk, Safety & Uncertainty Quantification, ETH Zurich, 2019, pp. 2–104. Report UQLab-V1.
[25] S. Marelli, C. Lamas, K. Konakli, C. Mylonas, P. Wiederkehr, B. Sudret, UQLab User Manual – Sensitivity Analysis, Chair of Risk, Safety and Uncertainty Quantification, ETH Zurich, Switzerland, 2019, pp. 3–106. Report # UQLab-V1.
[26] G. Blatman, Adaptive Sparse Polynomial Chaos Expansions for Uncertainty Propagation and Sensitivity Analysis, (PhD Thesis), Université Blaise Pascal, Clermont-Ferrand, 2009.
[27] B. Sudret, Global sensitivity analysis using polynomial chaos expansions, Reliab. Eng. Syst. Saf. 93 (2008) 964–979.
[28] R. Macian, M.A. Zimmermann, R. Chawla, Statistical uncertainty analysis applied to fuel depletion calculations, J. Nucl. Sci. Technol. 44 (2007) 875–885.
[29] S. Marelli, B. Sudret, An active-learning algorithm that combines sparse polynomial chaos expansion and bootstrap for structural reliability analysis, Struct. Saf. 75 (2018) 67–74.